NANO LETTERS

2009
Vol. 9, No. 2
590-594

Optical Absorption and Thermal Transport of Individual Suspended Carbon Nanotube Bundles

I-Kai Hsu,[†] Michael T. Pettes,[‡] Adam Bushmaker,[§] Mehmet Aykol,[§] Li Shi,[‡] and Stephen B. Cronin*[,§]

Department of Materials Science and Department of Electrical Engineering, University of Southern California, Los Angeles, California 90089, and Department of Mechanical Engineering and Center for Nano and Molecular Science and Technology, Texas Materials Institute, University of Texas at Austin, Austin, Texas 78712

Received September 10, 2008; Revised Manuscript Received December 4, 2008

ABSTRACT

A focused laser beam is used to heat individual single-walled carbon nanotube bundles bridging two suspended microthermometers. By measurement of the temperature rise of the two thermometers, the optical absorption of 7.4−10.3 nm diameter bundles is found to be between 0.03 and 0.44% of the incident photons in the 0.4 μm diameter laser spot. The thermal conductance of the bundle is obtained with the additional measurement of the temperature rise of the nanotubes in the laser spot from shifts in the Raman G band frequency. According to the nanotube bundle diameter determined by transmission electron microscopy, the thermal conductivity is obtained.

The electronic, optical, and thermal characterization of individual carbon nanotubes (CNTs) has evolved to an unprecedented level of sophistication.[1−3] In early work, bulk quantities of nanotubes were measured, yielding ensemble averages of measured properties.[4−10] Because of the strong chirality dependence of the physical properties of nanotubes, new measurement techniques were developed to characterize this important material on the individual nanotube level.[1−3,11−14] For example, Raman spectroscopy of individual carbon nanotubes has enabled the direct correlation between their physical structure and optical properties.[2] Similarly, combined optical and electronic measurements of individual carbon nanotubes have revealed a striking electron scattering mechanism by nonequilibrium phonon populations.[15,16] Despite these sophisticated techniques, many of the unique properties of nanotubes still elude us. For instance, their large surface-to-volume ratio strongly affects the ability to absorb and scatter light. Many aspects of this process, including surface recombination[17] and exciton−phonon dynamics,[18] are not well understood.

In a recent publication, an optical method for measuring thermal transport in carbon nanotubes was demonstrated.[19] In this method, a focused laser spot is used to locally heat suspended carbon nanotubes while the resulting temperature rise in the nanotube was measured simultaneously from the Raman G band frequency shift.[20] While this technique provides detailed information of the thermal contact resistance and diffusive/ballistic nature of phonon transport, the amount of optical absorption in the nanotube from the incident laser is unknown. As a result, no quantitative values of the thermal conductivity or the thermal contact resistance could be extracted from the measured spatial temperature profile of the nanotube. A somewhat similar method was applied to suspended, single-layer graphene.[21,22] While these graphene measurements report exciting results, with thermal conductivity values exceeding those of carbon nanotubes, these results assumed 11−12% laser power absorption by the single atomic graphene layer. Recent measurements of the optical opacity of graphene show that the total optical absorption is actually much less than this value.[23] In this paper, we present a new method for measuring the optical heating in suspended nanostructures directly, without any assumptions on the optical absorption or electron transport.

As a demonstration of this method, we directly measure the optical absorption in individual suspended single-walled carbon nanotube (SWNT) bundles bringing two suspended microthermometers. It was found that between 3.07×10^{-4} and 4.38×10^{-3} of the incident photons were absorbed by 7.4−10.3 nm diameter nanotube bundles in the 0.4 μm diameter laser spot. This measurement also gives the thermal conductance of the bundle from the temperature rise of the

* Corresponding author. E-mail: scronin@usc.edu.
[†] Department of Materials Science, University of Southern California.
[‡] Department of Mechanical Engineering and Center for Nano and Molecular Science and Technology, Texas Materials Institute, University of Texas at Austin.
[§] Department of Electrical Engineering, University of Southern California.

10.1021/nl802737q CCC: $40.75
Published on Web 01/13/2009

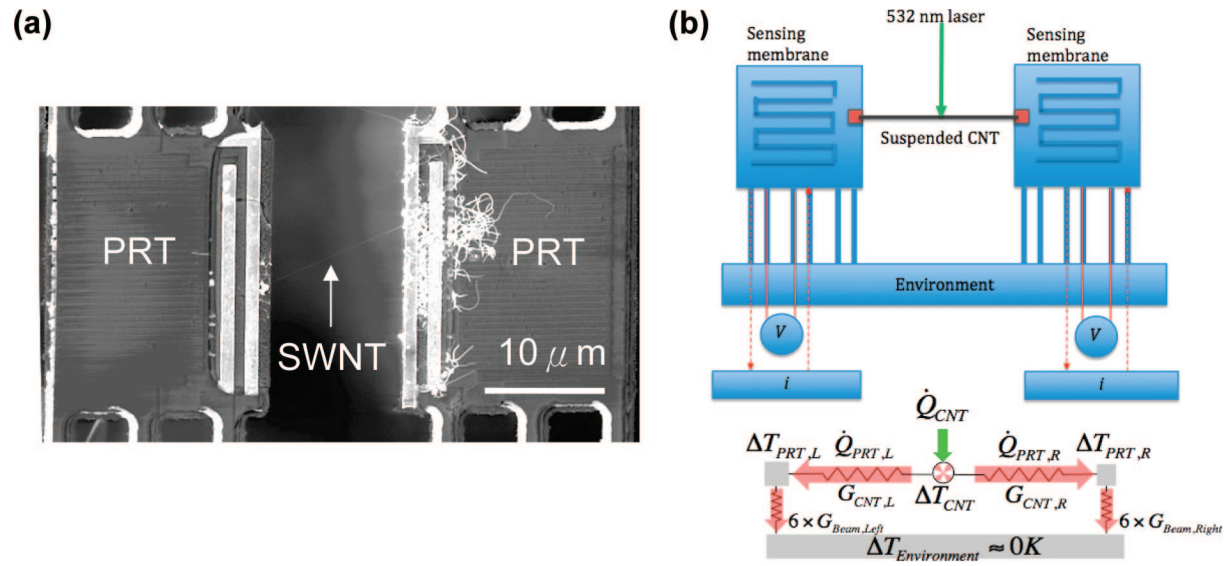

Figure 1. (a) Scanning electron microscopy image of microfabricated SiN_x membranes with platinum resistance thermometers (PRTs) bridged by a SWNT bundle. (b) Schematic diagram of the experimental setup and thermal resistance circuit.

nanotubes in the laser spot, determined from shifts in the G band Raman frequency.

In the experiment, a laser beam is focused on an individual carbon nanotube bundle suspended between two microfabricated thermometers, as shown in Figure 1a. The microfabricated platinum resistance thermometers (PRTs) consist of two adjacent 20 μm × 20 μm low-stress silicon nitride (SiN_x) membranes, each suspended by six 420 μm long and 2 μm wide SiN_x beams.[3] CNTs are grown by chemical vapor deposition across the two microfabricated thermometers. Details of the fabrication process of the microfabricated thermometers and CNTs are described in a previous publication.[3] The temperature dependence of the PRT devices are calibrated in a Linkam THMS temperature controlled stage. A 532 nm Spectra-Physics solid state laser is focused through a 100× objective lens with a numerical aperture of 0.9, producing a beam diameter of 0.4 μm full width at half-maximum (FWHM). A PRIOR ProScan II high-precision microscope stage is used to control the position of the incident laser spot. We focus the laser spot on the center of the carbon nanotube to reduce the unintentional heating of the microfabricated thermometers. The CNTs are aligned with the polarization of the incident laser. The laser power is varied from 300 to 1400 μW.

When the suspended carbon nanotube is irradiated with the focused laser, heat generated at the position of the laser spot will flow toward the two ends of the nanotube at lower temperature. On the basis of the thermal resistance circuit in Figure 1b, the power absorbed in the region of the incident laser spot ($\dot{Q}_{CNT}$) is equal to the sum of the power detected in both PRTs ($\dot{Q}_{PRT,L} + \dot{Q}_{PRT,R}$). This heat is detected by a small change in the resistance of the PRT with temperature ($\Delta R(T)$). The temperature coefficient of resistance of each PRT is calibrated by measuring its four-point resistance in a temperature-controlled stage. Once calibrated, we can convert any changes in the resistance of the PRTs to temperature changes due to heat conduction through the CNT bundles during laser exposure. Figure 1b shows a schematic diagram of the experimental configuration, together with a thermal circuit of the system. Two SR830 DSP lock-in amplifiers are connected to the outer two leads of each PRT with a sinusoidal current of 0.5 μA at a frequency of 200 Hz. The resolution in the resistance is around 1 Ω for a total resistance of approximately 30 kΩ. This corresponds to a heat flow of approximately 0.32 μW, which is much smaller than that created when the laser is incident on the carbon nanotube.

The power absorbed in the nanotube from the incident laser light depends on nanotube chirality, defect density, whether the CNT is an individual nanotube or in a bundle, and whether it has an electronic transition that is resonant with the incident laser energy. We can obtain the temperature of the CNT induced by laser heating from analysis of the Raman spectra, either from the anti-Stokes to Stokes Raman intensity ratio or from the downshift of the phonon bands.[24,25] Using the two microfabricated platinum thermometers (PRTs), supporting the suspended CNT at both ends, the temperature gradient can be determined from the temperatures observed in the CNT and the PRTs. Heat losses along the length of the nanotube due to radiation and air molecules are estimated to be 1 order of magnitude smaller than that due to conduction through the bundle.[26−29] Hence, the total power generated in the CNT by the incident laser is equal to the sum of the power detected in both PRTs.

Figure 2a shows a CNT bundle suspended across an 11 μm trench. The resistance of the thermometers is measured when the laser is both *on* and *off* the CNT in order to subtract any unintentional heating of the PRTs from the Gaussian tail of the incident laser spot hitting the SiN_x membrane. Accurate values of the resistance changes of both PRTs, solely due to the heat generated in the nanotube, can be obtained by subtracting the change in the resistance of the PRT with the laser spot *on* and *off* the CNT, as shown in Figures 2b and 2c. The relation between resistance change

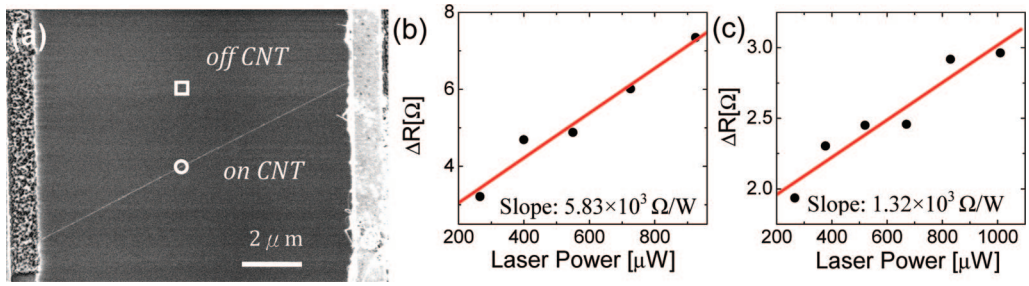

Figure 2. (a) Scanning electron microscopy image of a SWNT bundle suspended across an 11 μm trench. The circle and square represent the location of laser spot *on* and *off* the SWNT, respectively. (b, c) Resistance change with increasing laser power *on* and *off* the SWNT for the left and right thermometer, respectively.

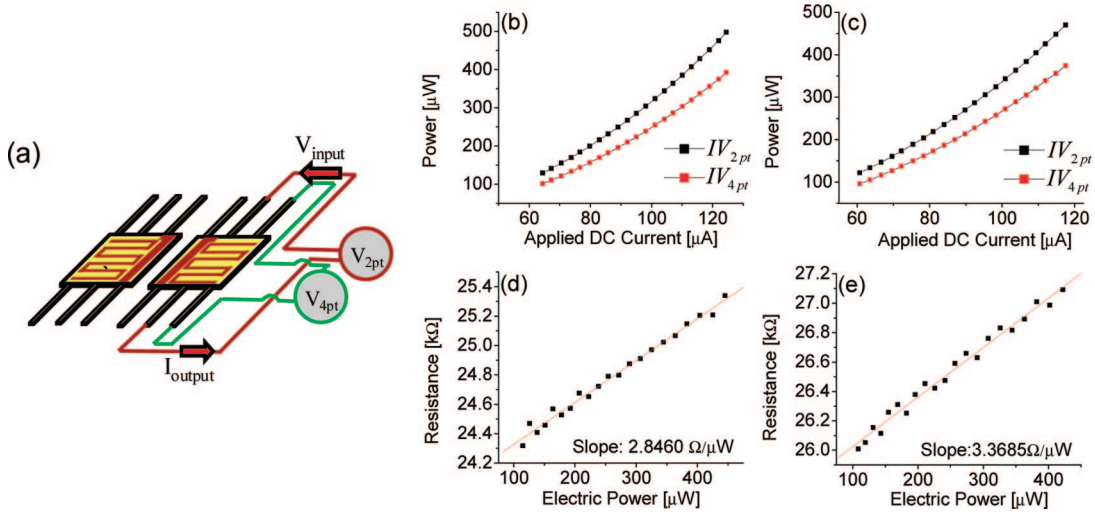

Figure 3. (a) Schematic diagram of the experimental setup for the PRT's electrical self-heating calibration. (b, c) Calibration data of the self-heating power plotted as a function of direct current for two-point and four-point measurements of the left and right PRTs. (d, e) Resistance of the left and right thermometers as a function of electric power, corrected for the effects of Joule heating in the leads.

Table 1. Data Summary of Four Measured CNT Bundles

sample	length of bundle (μm)	bundle diameter(nm)	no. of nanotubes in bundle	absorption probability	resonant Raman intensity (measd at 400 μW, 60 s)	thermal conductance (nW/K)	thermal conductivity (W/(m K))
1	11.7	N/A	N/A	2.4×10^{-3}	913	1.07	N/A
2	14.3	10.3	4	4.4×10^{-3}	3521	1.47	253
3	12.9	7.4	4	3.1×10^{-4}	928	2.28	683
4	12.3	8.2	5	1.6×10^{-3}	1050	0.51	118

and laser power is obtained from linear fits of these data, yielding values of 5.83×10^3 and 1.32×10^3 Ω/W for left and right thermometers, respectively. This factor of 4 difference in the heat conduction to the two thermometers is likely due to asymmetric thermal contact resistance.

In calibrating the PRTs, Joule heating is used to obtain the thermometer's resistance-power relation by applying a DC current. This is shown schematically in Figure 3a. In this calibration, heat is also generated in the two leads that supply current to the PRT device. Therefore, we must take into account the Joule heating in each lead ($\dot{Q}_{\mathrm{lead}}$) and the heat dissipated in the PRT ($\dot{Q}_{4\mathrm{pt}} = IV_{4\mathrm{pt}}$), observed by a four-point measurement. The power dissipated through one of the two leads can be obtained by subtracting the electric power measured by the two-point and four-point measurements of the PRT at elevated direct currents, $\dot{Q}_{\mathrm{lead}} = (IV_{2\mathrm{pt}} - IV_{4\mathrm{pt}})/2$. Since only half of the Joule heat generated in the leads causes heating in the PRTs and the other half is conducted to the substrate directly, we can write $\dot{Q}_{\mathrm{PRT}} = IV_{4\mathrm{pt}} + \dot{Q}_{\mathrm{lead}}$ for the heat flux into the PRT during this calibration. This relation is derived in detail elsewhere.[3] Figures 3d and 3e show the change in resistance with heating of the PRT ($\Delta R(\dot{Q}_{\mathrm{PRT}})$), corrected for the heat dissipation in the leads.

The heat generated in a nanotube bundle at a given laser power can be obtained by dividing the change in resistance ΔR observed under laser irradiation (Figures 2b and 2c) by the slopes in Figures 3d and 3e. The probability of laser photon absorption in a CNT is revealed by taking the ratio of the slopes in Figures 2b and 2c to the slopes of Figures 3d and 3e. It was found from this procedure that 2.05×10^{-3} and 3.92×10^{-4} of incident photon energy were conducted to the left and right thermometers, respectively. The total probability of nonradiative photon absorption in the CNT bundle is found by adding these two quantities, which yields 2.44×10^{-3}. Other samples measured, with diameters between 7.4 and 10.3 nm, exhibited absorption

probabilities between 3.07×10^{-4} and 4.38×10^{-3} when irradiated with the 0.4 μm diameter laser spot. If we try to correct for the small area of the nanotube bundle, by dividing by the area of nanotube that is irradiated (400 nm $\times$ 8 nm) and multiplying by the total irradiated area ($(\pi(200\text{ nm})^2$), we get absorptions of 1.2 and 17%, which are very high. However, this is not the correct way to define the absorption. Since photons are not localized below the diffraction limit, a photon passing 100 nm away from a resonant nanotube bundle can still be absorbed. We must, therefore, consider the total area of irradiation.

On the basis of the thermal resistance circuit shown in Figure 1b, the total absorbed laser power in the CNT is equal to the sum of the power flowing through both ends of the nanotube, as detected by the PRTs. This can be expressed as

$$\dot{Q}_{CNT} = \dot{Q}_{PRT,L} + \dot{Q}_{PRT,R} \tag{1}$$

in which

$$\dot{Q}_{PRT,L} = G_{CNT,L}(T_{CNT} - T_{PRT,L}) \tag{2}$$
$$\dot{Q}_{PRT,R} = G_{CNT,R}(T_{CNT} - T_{PRT,R})$$

where $G_{CNT,L}$ and $G_{CNT,L}$ are the thermal conductances of the nanotube segments to the left and right of the focused laser spot, respectively. We can express the conductance as and

$$G_{CNT,L} = \frac{\frac{\dot{Q}_{PRT,L}}{P_{Laser}}}{\frac{(T_{CNT} - T_{PRT,L})}{P_{Laser}}} \tag{3}$$

and

$$G_{CNT,R} = \frac{\frac{\dot{Q}_{PRT,R}}{P_{Laser}}}{\frac{(T_{CNT} - T_{PRT,R})}{P_{Laser}}}$$

where P_{Laser} is the incident laser power. Furthermore, the total conductance (G_{CNT}) of the CNT suspended between the two membranes is equal to $((G_{CNT,L})^{-1} + (G_{CNT,R})^{-1})^{-1}$.

The temperature of the CNT can be determined from Raman spectra taken from the scattered laser light. In particular, the G band Raman mode downshifts in frequency due to the thermal expansion of the carbon−carbon bond, which weakens the bond and lowers its vibrational frequency.[20] The temperature in the center of the suspended carbon nanotube shown in Figure 2, measured from the G band shifts, is shown in Figure 4a plotted as a function of laser power. Moreover, the temperatures of both PRTs are extracted from the resistance change and are shown in Figure 4b, based on the temperature coefficients of resistance, which are 3.24×10^{-4}/K and 3.73×10^{-4}/K for the left and right thermometers, respectively. The thermal resistance is obtained by dividing the temperature difference from the center to the end of the CNT per unit laser power by the optical absorption. The total thermal resistance of the carbon nanotube is obtained by summing these two serial thermal

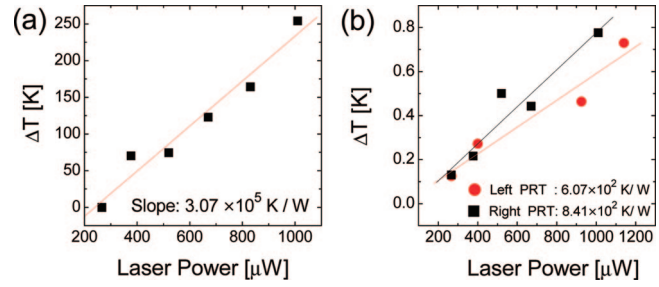

Figure 4. (a) Temperature in the center of the SWNT bundle shown in Figure 2 extracted from the G band downshifts plotted vs laser power. (b) Temperature of the left and right PRTs as a function of incident laser power.

resistances, which are 1.49×10^8 K/W and 7.83×10^8 K/W for the left and right segments, respectively, giving 9.32×10^9 K/W or a conductance of 1.07 nW/K.

We have performed these measurements on a total of four individual suspended nanotube bundles, listed in Table 1. The diameters and number of carbon nanotubes in each bundle for samples 2−4 are determined by high-resolution transmission electron microscopy (HRTEM). HRTEM images of the nanotube bundles measured in this study are shown in the Supporting Information. Sample 1 broke before HRTEM could be performed. The thermal conductance lies in the range from 0.51 to 2.28 nW/K, which is comparable to previous reports of Shi et al.[3] On the basis of the nanotube bundle diameters determined by HRTEM, the thermal conductivity varies from 118 to 683 W/m K. This low thermal conductivity can be attributed to internanotube coupling, defects, and thermal contact resistance between the nanotubes and the SiN_x membrane.

In conclusion, we demonstrate a technique that uses both Raman spectroscopy and microfabricated thermometers to determine the heat generated by the nonradiative absorption of light for suspended carbon nanotube bundles. Values for this absorption probability lie in the range from 3.07×10^{-4} to 4.38×10^{-3} for 7.4−10.3 nm diameter nanotube bundles. This is a direct measurement of the optical absorption of carbon nanotubes, in contrast to recent work on graphene, which measures the transmission but not the absorption.[23] Furthermore, this measurement gives the thermal conductance of the suspended nanostructures, based on the temperature gradient between the incident laser spot and the microthermometers. Upper and lower bounds of the thermal conductance are observed to be 0.51 and 2.28 nW/K. From the measured bundle diameters, thermal conductivity values between 118 to 683 W/m K are obtained. While this method has been demonstrated for carbon nanotube bundles, it is applicable to individual nanotubes and graphene with additional efforts to grow or assemble these nanostructures on the measurement device. The experimental results on optical absorption and optical heating in carbon nanotubes could find use in the exploration of different applications of nanotubes such as thermal cancer treatment therapy.[30]

Acknowledgment. This research was supported in part by DOE Award Nos. DE-FG02-07ER46376 and DE-FG02-07ER46377.

Supporting Information Available: High-resolution tunneling electron microscopy images of carbon nanotube bundles measured in this study. This material is available free of charge via the Internet at http://pubs.acs.org.

References

(1) Tans, S. J.; Devoret, M. H.; Dai, H. J.; Thess, A.; Smalley, R. E.; Geerligs, L. J.; Dekker, C. Individual single-wall carbon nanotubes as quantum wires. *Nature* **1997**, *386*, 474–477.

(2) Jorio, A.; Saito, R.; Hafner, J. H.; Lieber, C. M.; Hunter, M.; McClure, T.; Dresselhaus, G.; Dresselhaus, M. S. Structural (n, m) determination of isolated single-wall carbon nanotubes by resonant Raman scattering. *Phys. Rev. Lett.* **2001**, *86*, 1118–1121.

(3) Shi, L.; Li, D. Y.; Yu, C. H.; Jang, W. Y.; Kim, D. Y.; Yao, Z.; Kim, P.; Majumdar, A. Measuring thermal and thermoelectric properties of one-dimensional nanostructures using a microfabricated device. *J. Heat Transfer* **2003**, *125*, 881–888.

(4) Jorio, A.; Pimenta, M. A.; Souza, A. G.; Saito, R.; Dresselhaus, G.; Dresselhaus, M. S. Characterizing carbon nanotube samples with resonance Raman scattering. *New J Phys.* **2003**, *5*, 139.1139.17.

(5) Bockrath, M.; Cobden, D. H.; McEuen, P. L.; Chopra, N. G.; Zettl, A.; Thess, A.; Smalley, R. E. Single-electron transport in ropes of carbon nanotubes. *Science* **1997**, *275*, 1922–1925.

(6) Bachilo, S. M.; Strano, M. S.; Kittrell, C.; Hauge, R. H.; Smalley, R. E.; Weisman, R. B. Structure-assigned optical spectra of single-walled carbon nanotubes. *Science* **2002**, *298*, 2361–2366.

(7) Ebbesen, T. W.; Lezec, H. J.; Hiura, H.; Bennett, J. W.; Ghaemi, H. F.; Thio, T. Electrical conductivity of individual carbon nanotubes. *Nature* **1996**, *382*, 54–56.

(8) Dai, H. J.; Wong, E. W.; Lieber, C. M. Probing electrical transport in nanomaterials: Conductivity of individual carbon nanotubes. *Science* **1996**, *272*, 523–526.

(9) Hone, J.; Llaguno, M. C.; Nemes, N. M.; Johnson, A. T.; Fischer, J. E.; Walters, D. A.; Casavant, M. J.; Schmidt, J.; Smalley, R. E. Electrical and thermal transport properties of magnetically aligned single wall carbon nanotube films. *Appl. Phys. Lett.* **2000**, *77*, 666–668.

(10) Ruoff, R. S.; Lorents, D. C. Mechanical and Thermal-Properties of Carbon Nanotubes. *Carbon* **1995**, *33*, 925–930.

(11) Demczyk, B. G.; Wang, Y. M.; Cumings, J.; Hetman, M.; Han, W.; Zettl, A.; Ritchie, R. O. Direct mechanical measurement of the tensile strength and elastic modulus of multiwalled carbon nanotubes. *Mater. Sci. Eng., A* **2002**, *334*, 173–178.

(12) Pop, E.; Mann, D.; Wang, Q.; Goodson, K.; Dai, H. J. Thermal conductance of an individual single-wall carbon nanotube above room temperature. *Nano Lett.* **2006**, *6*, 96–100.

(13) Choi, T. Y.; Poulikakos, D.; Tharian, J.; Sennhauser, U. Measurement of the thermal conductivity of individual carbon nanotubes by the four-point three-omega method. *Nano Lett.* **2006**, *6*, 1589–1593.

(14) Yu, C. H.; Shi, L.; Yao, Z.; Li, D. Y.; Majumdar, A. Thermal conductance and thermopower of an individual single-wall carbon nanotube. *Nano Lett.* **2005**, *5*, 1842–1846.

(15) Pop, E.; Mann, D.; Cao, J.; Wang, Q.; Goodson, K.; Dai, H. J. Negative differential conductance and hot phonons in suspended nanotube molecular wires. *Phys. Rev. Lett.* **2005**, *95*, 155505.

(16) Bushmaker, A. W.; Deshpande, V. V.; Bockrath, M. W.; Cronin, S. B. Direct observation of mode selective electron-phonon coupling in suspended carbon nanotubes. *Nano Lett.* **2007**, *7*, 3618–3622.

(17) Uryu, S.; Ando, T. Exciton absorption of perpendicularly polarized light in carbon nanotubes. *Phys. Rev. B* **2006**, *74*, 155411.

(18) Misewich, J. A.; Martel, R.; Avouris, P.; Tsang, J. C.; Heinze, S.; Tersoff, J. Electrically induced optical emission from a carbon nanotube FET. *Science* **2003**, *300*, 783–786.

(19) Hsu, I. K.; Kumar, R.; Bushmaker, A.; Cronin, S. B.; Pettes, M. T.; Shi, L.; Brintlinger, T.; Fuhrer, M. S.; Cumings, J. Optical measurement of thermal transport in suspended carbon nanotubes. *Appl. Phys. Lett.* **2008**, *92*, 063119.

(20) Chiashi, S.; Murakam, Y.; Miyauchi, Y.; Maruyama, S. Temperature dependence of Raman scattering from single-walled carbon nanotubes: Undefined radial breathing mode peaks at high temperatures. *Jpn. J. Appl. Phys.* **2008**, *47*, 2010–2015.

(21) Ghosh, S.; Calizo, I.; Teweldebrhan, D.; Pokatilov, E. P.; Nika, D. L.; Balandin, A. A.; Bao, W.; Miao, F.; Lau, C. N. Extremely high thermal conductivity of graphene: Prospects for thermal management applications in nanoelectronic circuits. *Appl. Phys. Lett.* **2008**, *92*, 151911.

(22) Balandin, A. A.; Ghosh, S.; Bao, W. Z.; Calizo, I.; Teweldebrhan, D.; Miao, F.; Lau, C. N. Superior thermal conductivity of single-layer graphene. *Nano Lett.* **2008**, *8*, 902–907.

(23) Nair, R. R.; Blake, P.; Grigorenko, A. N.; Novoselov, K. S.; Booth, T. J.; Stauber, T.; Peres, N. M. R.; Geim, A. K. Fine structure constant defines visual transparency of graphene. *Science* **2008**, *320*, 1308–1308.

(24) Raravikar, N. R.; Keblinski, P.; Rao, A. M.; Dresselhaus, M. S.; Schadler, L. S.; Ajayan, P. M. Temperature dependence of radial breathing mode Raman frequency of single-walled carbon nanotubes. *Phys. Rev. B* **2002**, *66*, 235424.

(25) Jinno, M.; Ando, Y.; Bandow, S.; Fan, J.; Yudasaka, M.; Iijima, S. Raman scattering study for heat-treated carbon nanotubes: The origin of approximate to 1855 cm^{-1} Raman band. *Chem. Phys. Lett.* **2006**, *418*, 109–114.

(26) The Rayleigh number for this geometry is calculated to be on the order of 10^{-14} to 10^{-15}, which is much smaller than the typical range between 10^{-6} and 10^{12} for natural convection to occur. For such a small Rayleigh number approaching zero, free convection is negligible and the heat loss to air is dominated by heat conduction.[28] Because the carbon nanotube diameter is much smaller than the mean free path of air molecules, molecular gas conduction should be calculated using detailed gas dynamics instead of Fourier's law. When the molecule accommodation coefficient is 1, the molecular thermal conductance per unit nanotube length reaches the upper bound of $g = (nv/4)(3k_B/2)(\pi d) \approx 0.2$ mW/(m·K) for a 10 nm diameter (d) nanotube bundle, where n and v are the number density and mean velocity of air molecules, respectively, and k_B is the Boltzmann constant.[29] The average temperature rise in the nanotube is about half of the temperature at the laser spot, or $\Delta T \approx 100$ K. For a nanotube of length $L = 10$ μm, the heat loss to air molecules is $q < g\Delta TL \sim 0.2$ μW, which is 1 order of magnitude smaller than the absorbed laser power transferred by conduction along the nanotube to the two membranes. On the other hand, radiation heat loss from the nanotube is estimated to be 3 orders of magnitude smaller than the absorbed laser power.

(27) Mills, A. F., *Heat Transfer*; Prentice Hall: Upper Saddler River, NJ, 1999.

(28) Linan, A.; Kurdyumov, V. N. Laminar free convection induced by a line heat source, and heat transfer from wires at small Grashof numbers. *J. Fluid Mech.* **1998**, *362*, 199–227.

(29) Mann, D.; Pop, E.; Cao, J.; Wang, Q.; Goodson, K.; Dai, H. J. Thermally and molecularly stimulated relaxation of hot phonons in suspended carbon nanotubes. *J. Phys. Chem. B* **2006**, *110*, 1502–1505.

(30) Chakravarty, P.; Marches, R.; Zimmerman, N. S.; Swafford, A. D. E.; Bajaj, P.; Musselman, I. H.; Pantano, P.; Draper, R. K.; Vitetta, E. S. Thermal ablation of tumor cells with anti body-functionalized single-walled carbon nanotubes. *Proc. Natl. Acad. Sci. U.S.A.* **2008**, *105*, 8697–8702.

NL802737Q